LETTERS

The purpose of this Letters section is to provide rapid dissemination of important new results in the fields regularly covered by The Physics of Fluids. Results of extended research should not be presented as a series of letters in place of comprehensive articles. Letters cannot exceed three printed pages in length, including space allowed for title, figures, tables, references and an abstract limited to about 100 words.

The growth of swirl in curved circular pipes

D. E. Olson and B. Snyder
Pulmonary Disease Unit, Veterans Adminstration Medical Center/University of Michigan, Ann Arbor, Michigan 48105

(Received 1 November 1982; accepted 6 December 1982)

Steady secondary currents in the entry region of curved circular pipes with different curvature ratios ($R/a = 4.66$ and 16) have been delineated at moderate Dean numbers by pulsed-probe anemometry. When swirl is quantified using circulation loops, flow development can be scaled by the length parameter $(aR)^{1/2}$. The initial growth of axial swirl seems consistent with a model of vorticity transport based on average streamline curvature, but does not progress monotonically to an asymptotic value. Instead, an abrupt relaxation occurs approximately $2(aR)^{1/2}$ downstream from the inlet, suggesting that boundary-layer current intensifies well before the axial velocity profile can be reordered by convection.

Recent experimental[1,2] and theoretical[3] studies show that two length scales are required to characterize the development of steady flow in curved circular pipes at moderate Dean number $K = 2(a/R)^{1/2}(a\bar{W}/\nu)$, where (R/a) is the pipe curvature ratio and $2(a\bar{W}/\nu)$ the Reynolds number. Each length scale describes a region in which a specific mechanism dominates flow development in curved pipes. Agrawal *et al.*[1] reasoned that vorticity dynamics require the onset of strong secondary currents within an entrance region of "upstream influence" extending through the initial few pipe diameters. Yao and Berger[3] showed theoretically that this upstream length could be scaled as $(aR)^{1/2}$. By contrast, the completion of flow development has been predicted to occur throughout an extended region of "downstream influence" governed by boundary-layer growth, scaled to a length of order $(aRK)^{1/2}$. Experimental studies[1,2] of secondary flows in curved pipes demonstrate the presence of upstream and downstream regions, but do not substantiate the proposed length scales, nor quantify the growth of secondary currents.

A quantitative model of vorticity transfer[4,5] predicts the growth of secondary streamwise vorticity ξ along a streamline having curvature R and located at an angle $(\pi/2 - \phi)$ out of the symmetry plane to be given by

$$\xi = -2\theta\Omega\cos\phi, \tag{1}$$

where Ω is the inlet azimuthal vorticity and $\theta\,(= L/R)$ is the deflection of the streamline over a path length L. As this model neglects viscous effects and streamline displacement, Eq. (1) can be applied only in an upstream region, length of order R. In this letter, we report measured growth rates of ξ in the boundary layer and inviscid central core, under conditions of laminar airflow at moderate K. Uniform inlet velocity profiles were used to ascertain whether Eq. (1) can predict the upstream influence of an inlet vortex ring on the development of flow in a bend.

Two circular curved pipes were machined from Plexiglas in half-sections, using a semicircular cutter to ensure 1% geometric accuracy. Both pipes were 3.81 cm i.d., extended through 300° of arc, and had curvature ratios R/a of 4.66 or 16. An axial fan supplied steady, low-pressure airflow which was stabilized by passage through an upstream plenum and heat exchanger. Volume flow rates were measured by rotameters to within $\pm$ 1% accuracy. Inlet flows were screened and straightened, then shaped by an entrance bell to produce nearly flat entrance profiles that had no detectable secondary currents. Inlet axisymmetric vortex rings were confined to a wall region $0.25a$ in thickness.

Transverse (X-, Y-) and axial (Z-) velocity components were measured at selected downstream intervals, using a pulsed-probe anemometer[6] protruding into the flow stream through tightly fitted slots milled into the pipe wall. The probe tip was positioned by a micromanipulator at intervals of $0.1a$ along the five vertical (Y-axis) and five horizontal (X-axis) traverses shown in Fig. 1. Along each traverse the magnitude and direction of pointwise velocities were found by rotating the probe tip until the velocity signal was maximal. All three pointwise components were then interpolated throughout the grid of Fig. 1 by simultaneous solution of linear equations. These data were supplemented by measurements of total velocity within the boundary annulus extending 1 mm from the pipe wall, using a conventional hot-wire anemometer. The resulting traces were then least-squares-fitted to a four-term Fourier series to obtain transverse velocity profiles, as shown in Fig. 1.

Preliminary testing[2] demonstrated probe position to be resolved to within $\pm$ 0.5 mm and direction to within $\pm$ 0.5°. Although the probe shaft obstructed up to 3% of the flow cross section, pointwise velocities usually were repeatable to within 5% when the probe was inserted from opposite walls of the pipe, and symmetric to the same degree about the X

 0031-9171/83/020347-03$01.90

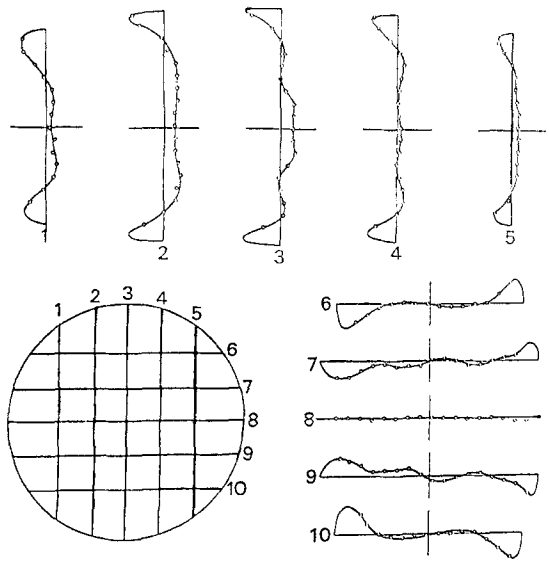

FIG. 1. Configuration of vertical (1–5) and horizontal (6–10) probe traverses, with corresponding X and Y components of secondary velocity. Inner wall of pipe bend is towards the left. Parabolic inlet velocity profile, $R/a = 4.66$, Re = 1030, at 180° of bend. Length and velocity scales: each interval between traverses $= 0.3a = 0.3\overline{W}$ cm/sec.

axis. Therefore we infer that all secondary velocities were determined to within 5% accuracy.

Secondary currents at downstream intervals were delineated at Re of 300 and 1030, for each curvature ratio. Flow patterns generated at the higher Re are presented in Figs. 2(a) and 2(b) for R/a of 4.66 and 16, respectively. In all cases the most prominent feature is the strong boundary-layer current already present 20° into the bend, in accord with previous observations.[1] This secondary current initially is strongest along the vertical axis, but at 40°–60° clearly favors the inner wall (compare P to P' in Fig. 2). This shift coincides with a pronounced increase in azimuthal velocity. Downstream, the point of maximal current reverts to the Y axis, while peak secondary velocities diminish as much as twofold. Hence this secondary current "overshoot" is typified by changes in both distribution and magnitude throughout the region of flow development. A similar "overshoot" in the axial velocity profile occurs concurrently.[1,2]

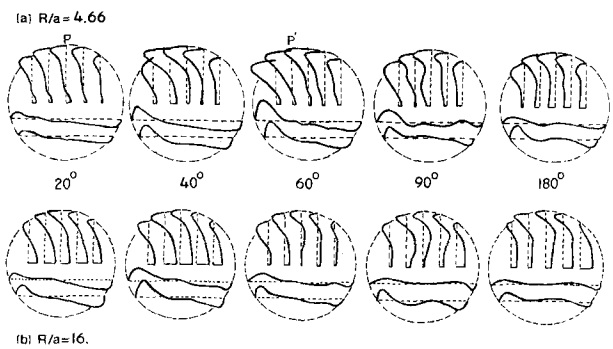

FIG. 2. X- and Y- secondary velocity profiles within the first 180° of curved pipes, flat inlet velocity profile, (a) $R/a = 4.66$, Re = 1030, $K = 475$; (b) $R/a = 16$, Re = 1030, $K = 260$. Note the reversal of central crossflows between 40° and 90° in (a), and the progressive shift in the position of peak boundary-layer current from P to P'. (All secondary velocities are normalized to the mean axial velocity $\overline{W} = 42$ cm/sec.)

Other evidence of kinematically similar development is less apparent. As seen in Fig. 2, the central crossflows evolve nonuniform, idiosyncratic motions[7]: in some instances crossflow even reverses, as Squire[8] and Hawthorne[8] inferred from measurements of total pressure. The circulating eddy of the more developed flow seen in Fig. 1 has a helical pitch,[9] defined as

$$\oint \Big((\text{local axial velocity})/(\text{local eddy velocity}) \Big)\, ds,$$

of about 25 diameters, which is consistent with Taylor's observations[9] of dye traces entrained in the boundary layer of fully developed curved flow. This measure suggests swirl to be surprisingly weak, because crossflows in the inviscid core are much smaller than the local axial velocities. Thus pitch is limited by the weak central crossflows, and insensitive to the strong boundary-layer currents.

These secondary currents are better quantified by defining circulation loops typical of the inviscid core, the "maximal" circulation, and the boundary layer. The maximal and boundary-layer paths [shown in Figs. 3(a) and 3(b) respectively] were chosen to maximize circulation, while the inviscid loop (not shown) was a fixed path centered in the core. The circulation integrals were evaluated using the approximation

$$\Gamma \equiv \oint \mathbf{v}\cdot\mathbf{ds} \simeq \sum_i (U_i \Delta x_i + V_i \Delta y_i),$$

where U_i and V_i are the mean X and Y velocities on the ith path segment $(\Delta x_i, \Delta y_i)$.

A pattern common to all the circulation loops emerges from these calculations: a rapid initial growth in average streamwise vorticity $\overline{\xi}$ ($= \Gamma$/loop area), leading to a pronounced overshoot in $\overline{\xi}$ within a characteristic length $2(aR)^{1/2}$ downstream of the inlet. Maximal circulation loops applied to Agrawal's published data yield estimates of $\overline{\xi}$ that agree at least qualitatively with these findings, as in Fig. 3(a). The occurrence of vorticity overshoot in both the boundary layer and inviscid core suggests that secondary motions in these two regions are tightly coupled. This common pattern observed over a range of Dean numbers also implies that the initial development of secondary currents is kinematically similar if entrance lengths are scaled to Yao's[3] "upstream" length scale $(aR)^{1/2}$. As our flow sections may have been too short to allow the completion of flow development, the asymptotic decline in $\overline{\xi}$ cannot be scaled to $(aRK)^{1/2}$.

In comparing these results with the predictions of Squire and Winter,[4] we note that inlet vortex rings were confined to the wall, so that Eq. (1) can be applied only to the growth of $\overline{\xi}$ within the boundary layer, of thickness δ. Consistent with this restriction, after a path deflection $\theta = L/R$,

$$\overline{\xi}_{\text{pred}} = -2\theta \int_{-\pi/2}^{\pi/2} \int_{a-\delta}^{a} \Omega W \cos\phi \, r \, dr \, d\phi \Big/ \int_{-\pi/2}^{\pi/2} \int_{a-\delta}^{a} W r \, dr \, d\phi \simeq -2\theta \langle \Omega \cos\phi \rangle, \qquad (2)$$

where $\langle\ \rangle$ represents an average taken over $-\pi/2 \leqslant \phi \leqslant \pi/2$. The quantity $\langle \Omega \cos\phi \rangle$ was estimated by measuring inlet

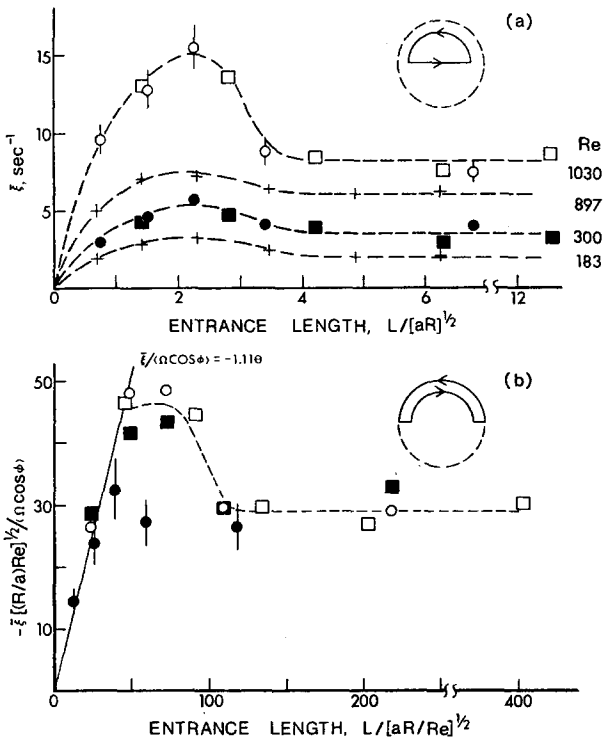

FIG. 3. Development of mean axial vorticity $\bar{\xi} = \Gamma/$(loop area): (a) on maximal circulation path; (b) in boundary layer. Solid line denotes the region of inviscid growth in $\bar{\xi}$. Error margins shown are representative of all data. $R/a = 4.66$: ● Re = 300, $K = 140$. ○ Re = 1030, $K = 475$. $R/a = 16$: ■ Re = 300, $K = 75$. □ Re = 1030, $K = 260$. + : Derived from data in Ref. 1, $R/a = 7$.

wall velocity gradients $\partial W/\partial r = \Omega$ at the entrance to the curved pipes. By Eq. (2) the ratio of experimental quantities $\bar{\xi}/\langle\Omega\cos\phi\rangle$, which indicates the relative strength of downstream axial vorticity, should equal -2θ. The resulting experimental ratios are presented in Fig. 3(b), using an axial length scale $(aR)^{1/2}/\mathrm{Re}^{1/2}$ to reconcile upstream inviscid transport and downstream viscous effects.

As Squire's analysis assumes inviscid flow and neglects boundary-layer growth we expect $\bar{\xi}_{\mathrm{pred}}$ in Eq. (2) to overestimate our experimental values, but the empirical ratio $\bar{\xi}/\langle\Omega\cos\phi\rangle$ still grows linearly with θ, as is evident in Fig. 3(b). The initial slope represents a regime of inviscid growth, $-(1.11 \pm .08)\theta$, describing all four cases through at least $\theta = 20°$. In the "asymptotic" region downstream of the overshoot, $\bar{\xi}$ decreases to $-(29 \pm 3)(R/a)^{-1/2}(\mathrm{Re})^{-1/2} \times \langle\Omega\cos\phi\rangle$. Thus we conclude that overshoot may occur because Squire's mechanism permits the build-up of intense boundary-layer currents long before the axial profile can be restructured by convection.

A prominent overshoot in streamwise secondary vorticity seems to be characteristic of flow development in tightly curved pipes with flat inlet velocity profiles. Its onset and initial linear growth is explicable through Squire's mechanism of vorticity transport as decribed by Eq. (1). The rapid growth in vorticity by inviscid mechanisms to a peak value near $2(aR)^{1/2}$ supports the utility of $(aR)^{1/2}$ as an upstream length scale. How axial velocity profiles and secondary currents interact to dampen this flow structure is as yet unclear.

Viewed as an initial-value problem, the rapid development of vorticity demonstrates that swirl intensity in short curved pipes is quite sensitive to the distribution of inlet vorticity. This has special pertinence to biological flow systems that are composed of repeatedly branching conduits. Within the curved segments connecting the branched conduits convective mixing must depend critically on conduit length and inlet vorticity. Some authors have proposed that head losses in such bends should be lower than in developed flow, but our results suggest otherwise. A "favorable" distribution of inlet vorticity can cause upstream boundary layer currents to be significantly more intense than asymptotic swirl, with head losses predicted to be correspondingly greater.

[1]Y. Agrawal, L. Talbot, and K. Gong, J. Fluid Mech. **85**, 497 (1978).
[2]D. E. Olson, Ph.D. thesis, University of London, 1971.
[3]L-S. Yao and S. A. Berger, J. Fluid Mech. **67**, 177 (1975).
[4]H. B. Squire and K. G. Winter, J. Aeronaut. Sci. **18**, 271 (1951).
[5]W. R. Hawthorne, *Proceedings of the Seminar on Aeronautical Sciences* (National Aeronautics Laboratory, Bangalore, India, 1961), pp. 307–333.
[6]This device, which can detect flow reversal, is discussed in Ref. 2. Pointwise velocities are determined by measuring the transport time and direction of a thermal pulse initiated at an upstream wire and sensed at a downstream wire.
[7]Possibly because inlet vorticity was not as closely confined to the pipe walls as in Agrawal's experiments, some details of the secondary flow were found to be quite sensitive to the inlet velocity distribution.
[8]See Ref. 5, pp. 319–324.
[9]Helical pitch is defined by Taylor as the axial length required for a fluid parcel entrained in an eddy to trace a complete circuit. G. I. Taylor, Proc. R. Soc. London Ser. A **124**, 243 (1929).